Available online at www.sciencedirect.com
SCIENCE DIRECT®
Journal of Organometallic Chemistry 691 (2006) 53–58
Journal of Organometallic Chemistry
www.elsevier.com/locate/jorganchem

Empirical analysis of bonding in ferrocenes

Igor Novak [a,*], Branka Kovač [b]

[a] Charles Sturt University, Orange NSW 2800, Australia
[b] Physical Chemistry Division, "R. Bošković" Institute, HR-10000 Zagreb, Croatia

Received 27 July 2005; received in revised form 1 September 2005; accepted 1 September 2005
Available online 6 October 2005

Abstract

HeI and HeII photoelectron spectra (UPS) of 1-cyanomethyl, 1-butyryl and 1,1′-bis(dimethylsilyl)-ferrocene were measured. The nature of metal–ligand bonding was analyzed via regression analysis of UPS related experimental descriptors.
© 2005 Elsevier B.V. All rights reserved.

Keywords: Photoelectron spectroscopy; Ferrocenes; Bonding

1. Introduction

Ferrocene derivatives are important because of their applications in catalysis and material science [1]. Numerous studies describing their electronic structure and the nature of metal–ligand bonding have been published. Some studies used theoretical methods to investigate photoionization and photoexcitation processes in the parent ferrocene [2,3]. Others used UV photoelectron spectroscopy (UPS) to probe the nature of metal–ligand bonding in ferrocenes [4–12]. UPS was found to be a very suitable method especially when studies were performed at variable photon energies [10]. In this work, we present HeI/HeII photoelectron spectra of three ferrocenes whose spectra have not been reported previously. The ferrocenes were selected because they could be vaporized by heating without decomposition and contain ring substituents which complement those of ferrocenes studied previously (Table 2). We describe new approach to the study of bonding which relies on the correlation analysis of experimental descriptors pertinent to ligand and metal orbitals rather than on various theoretical models and calculations.

2. Experimental and computational

The sample compounds: 1-cyanomethyl-ferrocene (**1**), ferroceneacetonitrile (**2**) and 1,1′-bis(dimethylsilyl)-ferrocene (**3**) were obtained from Sigma–Aldrich and their identity checked by HPLC, melting point measurements and elemental analysis.

Photoelectron spectra were recorded on Vacuum Generators UV-G3 spectrometer and calibrated with small amounts of Xe gas which was added to the sample flow. The sample temperatures were 100, 100 and 60 °C for **1**–**3**, respectively.

DFT calculations were performed with GAUSSIAN 03 software [13] using B3LYP functional and pseudorelativistic, effective core potential basis set [14] for Fe and 6-31G* set for other atoms. In the calculations, the geometry was fully optimized at B3LYP level. Older [15] and recent [3] work have pointed out that the Koopmans approximation is inadequate for analyzing UPS of ferrocenes. Therefore, the first vertical ionization energy (E_1) was calculated by subtracting the total electron energy for the optimized, neutral molecule from the energy of the molecular ion with the same geometry. Higher vertical ionization energies were then calculated by TDDFT method which gives excitation energies for the molecular ion. The excitation energies added to IE_1 then gave approximate values for higher

* Corresponding author.
E-mail address: inovak@csu.edu.au (I. Novak).

0022-328X/$ - see front matter © 2005 Elsevier B.V. All rights reserved.
doi:10.1016/j.jorganchem.2005.09.001

ionization energies. A similar approach was used previously [12a].

3. Results and discussion

The HeI and HeII photoelectron spectra are shown in Figs. 1–3 and the assignments are summarized in Table 1. The low energy region of the spectra (<11 eV) can be assigned by comparison with the spectra of ferrocene [5], substituted ferrocenes [6–9] and DFT calculations. As the results in Table 1 indicate the absolute differences between calculated and measured ionization energies are <0.5 eV which is comparable to Greens Functions method which is the standard method for the assignment of photoelectron spectra. The two lowest band manifolds (X–B) and (C–F) correspond to ionization from Fe3d and cyclopentadienyl (Cp) ligand orbitals, respectively. These orbitals are related to $e_2' + a_1'$ and $e_1' + e_1''$ orbitals in the parent ferrocene. The bands at 10.45 and 10.85 eV in the spectrum of **3** correspond to ionizations from Si–C σ-orbitals as can be ascertained by comparison with the spectra of silicone bridged ferrocenophanes [12a]. Band at 11.85 eV in the spectrum of **1** can be attributed to ionization from π_{CN} orbital on the basis of comparison with CH_3CN spectrum [12b]. Relative intensities of the first two band manifolds are listed in Table 1. Relative intensity of the first manifold (Fe3d ionization) increases on going from HeI to HeII excitation. Similar intensity increase has also been observed in other ferrocene derivatives and can be related to the shape resonance observed in photoionization cross-section of metallocenes at 40 eV photon energy [10]. The resonance is most apparent in the photoionization from orbitals with 3d metal character. Its presence in the continuum profile of external valence bands of metallocenes provides support for the interpretation of relative band intensity increase on going from HeI to HeII radiation as being characteristic of the initial state with metal 3d character. The measured intensity ratios of Cp vs. Fe3d manifolds (2.47) differ from

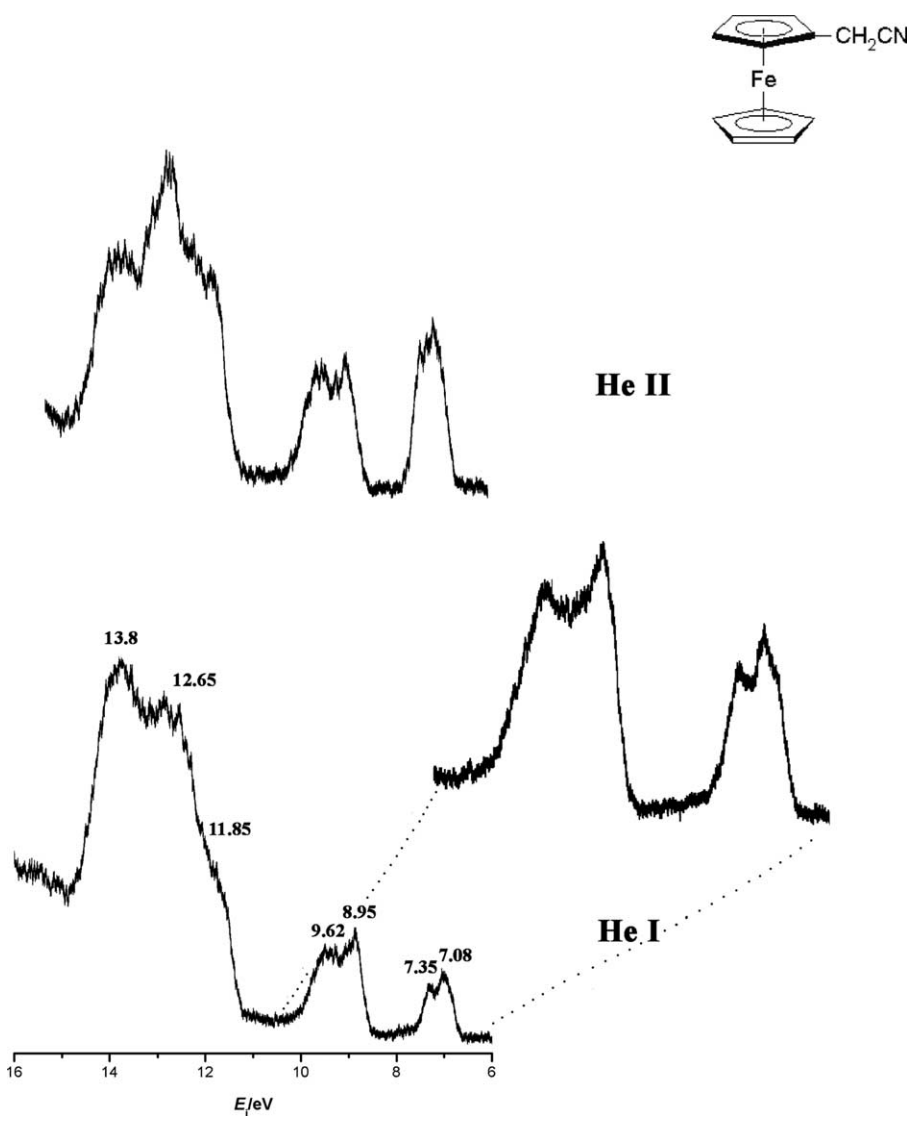

Fig. 1. HeI and HeII photoelectron spectra of **1**.

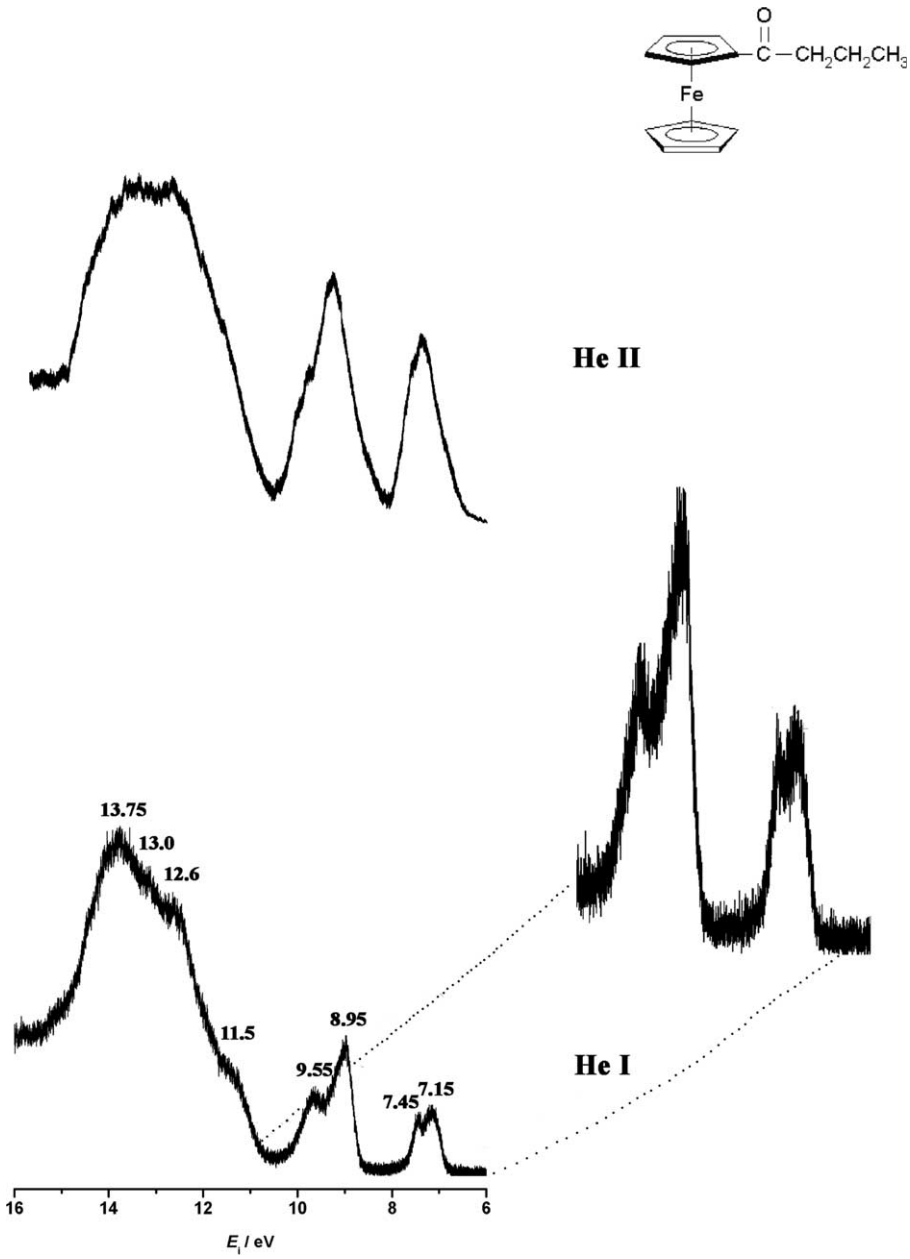

Fig. 2. HeI and HeII photoelectron spectra of **2**.

the statistical ratio which is 4/3. The difference can be attributed to photoionization cross-section ratio of C2p/Fe3d orbitals which is 6.12/4.83 at HeI photon energy [16].

The substitution of cyclopentadienyl ring influences the first E_i of ferrocenes as can be seen from Table 3. The presence of electron-withdrawing substituents (e.g., halogens, alkoxy, cyano or acetyl groups) leads to increase in the first vertical ionization energy vs. parent ferrocene. The presence of formally electron donating groups (e.g., alkyl, alkylsilyl, methoxy groups) leads to decrease in ionization energy. The presence of phenyl or benzyl groups also leads to a decrease in the first ionization energies. However, the effect of alkylsilyl substitution is smaller than that of phenyl or benzyl groups. The substituent effects appear to be cumulative and linear (at least for disubstituted ferrocenes). For example, the increase in first ionization energy for 1,1′-dichloroferrocene is twice as large as for chloroferrocene.

The following descriptors were used in the electronic structure analysis: individual Fe3d ionization energies and their average ⟨3d⟩, π-ionization energies from Cp moiety (π_2,π_1), ^{57}Fe NMR chemical shifts (δ) [17,18] and Hammett substituent constants (σ) [19]. The substitution of Cp ring leads to a reduction of molecular symmetry and subsequent splitting of Cp π-orbital levels (π_2,π_1) which in parent ferrocene have symmetries e_1' and e_1''. The ligand π-ionization energies used as descriptors were averages of split components. The values of descriptors are given in Tables 2 and 3. In order to understand how substituents affect the electronic structure and bonding we performed linear

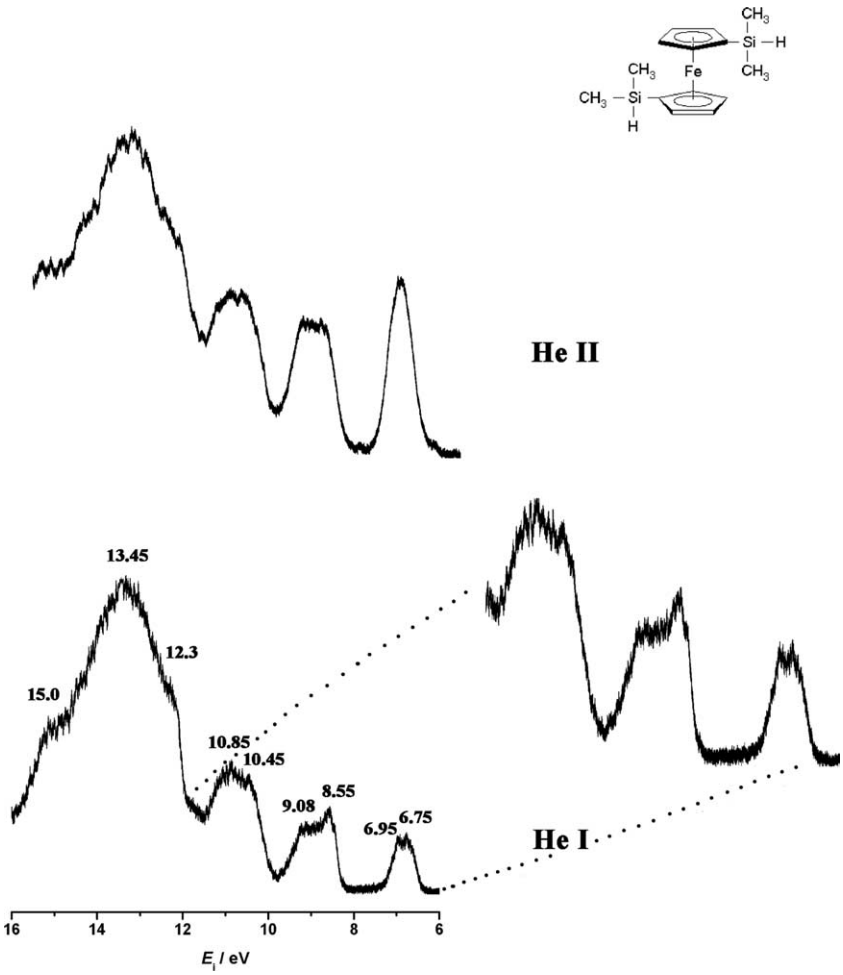

Fig. 3. HeI and HeII photoelectron spectra of **3**.

Table 1
Vertical ionization energies E_i, calculated ionization energies (TDDFT), band assignments and relative band intensities[a]

Molecule	Band	$E_i \pm 0.2$ (eV)	TDDFT (eV)	Assignment	HeII/HeI intensity ratio
1	X–B	7.08, 7.35	7.30, 7.76, 8.0	Fe3d	1.0
	C–F	8.95, 9.62	8.50, 9.27, 9.28, 9.82	π_{Cp}	0.53
	D	11.85		π_{CN}	
2	X–B	7.15, 7.45	7.31, 7.71, 7.97	Fe3d	1.0
	C–G	8.95, 9.55	8.49, 9.42, 9.70	π_{Cp}, n_O	0.66
	H	11.5		π_{CO}	
3	X–B	6.75–6.95	6.70, 7.14, 7.25	Fe3d	1.0
	C–F	8.55, 9.08	8.6, 9.02, 9.13	π_{Cp}	0.55
	G–H	10.45, 10.85		σ(Si–C)	

[a] Only bands below 12 eV are listed since bands at higher ionization energies overlap strongly and also because TDDFT method becomes unreliable for transition energies >5 eV.

regression analyses on suitable pairs of descriptors. The standard deviations (SD) and correlation coefficients (R) are given in Table 4.

The results in Table 4 show that the correlation between individual Fe3d energies or ⟨3d⟩ on the one hand and NMR chemical shifts (δ) on the other is poor. This is in accord with the known fact that changes in chemical shifts of transition metals are affected by paramagnetic shielding term [20]. Paramagnetic shielding depends not only on the electron density at the metal nucleus, but also on other terms which are due to nephelauxetic effect of the ligands. The influence of individual terms cannot be readily deduced from experimental parameters. This complicated dependence leads to poor correlation between Fe3d energies and chemical shifts, because ionization energies of Fe3d are dominated by the electron density at the iron

Table 2
Average ionization energies (eV) and ^{57}Fe NMR data (δ)[a,b]

Substituent	⟨3d⟩	⟨π_2⟩	⟨π_1⟩	δ (ppm)
H[(6)]	6.97	8.77	9.28	0.0
Cl[(6)]	7.14	8.90	9.50	−1.2[(17)]
1,1′-Cl[(6)]	7.33	8.96	9.63	
1,1′-Br[(6)]	7.29	8.86	9.57	
1, 1′-CH_3[(8)]	6.87	8.59	9.12	
1, 1′-C_2H_5[(7)]	6.71	8.46	9.05	69.2[(17)]
–$(CH_2)_3CH_3$[(8)]	6.85	8.59	9.21	
–$C(CH_3)_3$[(8)]	6.80	8.56	9.17	38.1[(17)]
–$(CH_2)_4CH_3$[(8)]	6.83	8.57	9.18	
–CH_2CN*	7.17	8.95	9.62	−1.2[(17)]
1,1′-CN[(7)]	7.96	9.67	10.27	
–CH=CH_2[(8)]	6.96	8.89	9.29	165.8[(17)]
Z–CH=CH–CN[(9)]	7.31	8.97	9.60	
E–CH=CH–CN[(9)]	7.38	9.00	9.66	
–CHO[(8)]	7.40	9.08	9.75	232.5[(17)]
–$COCH_3$[(8)]	7.30	9.05	9.74	234.2[(17)]
–$CO(CH_2)_2CH_3$*	7.25	8.95	9.55	
–CH_2NMe_2[(8)]	6.98	8.74	9.33	0.5[(17)]
–CH_2OH[(8)]	7.13	8.85	9.61	−1.2[(17)]
–COOMe[(8)]	7.21	8.91	9.65	194.7[(17)]
–C_6H_5[(11)]	6.84	8.02	8.73	188.1[(17)]
1, 1′-OCH_3[(7)]	6.67	8.23	9.04	
1, 1′-$COCH_3$[(7)]	7.43	9.17	9.78	436.9[(17)]
1, 1′-$OOCCH_3$[(7)]	6.91	8.63	9.27	
1, 1′-$COOCH_3$[(7)]	7.26	8.95	9.68	379.8[(17)]
1, 1′-$CH_2C_6H_5$[(7)]	6.67	8.32	8.94	
1, 1′-C_6H_5[(7,11)]	6.80	7.92	9.00	
1, 1′-$SiHMe_2$*	6.82	8.55	9.08	170.3[(18)]
–$(C_2H_5)_{10}$[(5)]	6.01	7.31	8.08	

[a] Compounds designated by asterisk were studied in this work for the first time.
[b] Superscript numbers in brackets indicate references from which UPS and ^{57}Fe NMR data were taken.

Table 3
Fe3d ionization energy descriptors (eV) and Hammett substituent constants (σ)[a,b]

Substituent	3d (e_2')	3d (a_1')	$\Sigma\sigma^+$	$\Sigma\sigma^-$	$\Sigma\sigma_m$	$\Sigma\sigma_p$
H[(6)]	6.85	7.21	0.0	0.0	0.0	0.0
Cl[(6)]	7.02	7.38	0.11	0.19	0.37	0.23
1,1′-Cl[(6)]	7.21	7.58	0.22	0.38	0.74	0.46
1,1′-Br[(6)]	7.17	7.54	0.30	0.50	0.78	0.46
1, 1′-CH_3[(8)]	6.76	7.10	−0.62	−0.34	−0.12	−0.28
1, 1′-C_2H_5[(7)]	6.60	6.94		1.38	−0.14	−0.30
–$(CH_2)_3CH_3$[(8)]	6.74	7.08	−0.29	−0.12	−0.07	−0.16
–$C(CH_3)_3$[(8)]	6.69	7.03	−0.26	−0.13	−0.10	−0.20
–$(CH_2)_4CH_3$[(8)]	6.71	7.06		−0.19	−0.08	−0.15
–CH_2CN*	7.08	7.35	0.16	0.11	0.16	0.18
1,1′-CN[(7)]	7.85	8.18		1.76	1.12	1.32
–CH=CH_2[(8)]	6.85	7.19	−0.16		0.08	−0.08
Z–CH=CH–CN[(9)]	7.21	7.51				
E–CH=CH–CN[(9)]	7.27	7.59				
–CHO[(8)]	7.29	7.62		1.03	0.36	0.44
–$COCH_3$[(8)]	7.20	7.49		0.84	0.38	0.50
–$CO(CH_2)_2CH_3$*	7.15	7.45				
–CH_2NMe_2[(8)]	6.87	7.20	−0.49		0.11	−0.17
–CH_2OH[(8)]	7.03	7.34	−0.04	0.08	0.01	0.01
–COOMe[(8)]	7.10	7.44		0.75	0.32	0.39
–C_6H_5[(11)]	6.72	7.10	−0.18	0.02	0.06	−0.01
1, 1′-OCH_3[(7)]	6.55	6.91	−1.56	−0.52	0.22	−0.54
1, 1′-$COCH_3$[(7)]	7.36	7.58		1.68	0.76	1.0
1, 1′-$OOCCH_3$[(7)]	6.81	7.11	−0.38		0.78	0.62
1, 1′-$COOCH_3$[(7)]	7.17	7.45		1.5	0.64	0.78
1, 1′-$CH_2C_6H_5$[(7)]	6.57	6.87	−0.56	−0.18	−0.16	−0.18
1, 1′-C_6H_5[(7,11)]	6.63	6.97	−0.36	0.04	0.12	−0.02
1, 1′-$SiHMe_2$*	6.75	6.95				
–$(C_2H_5)_{10}$[(5)]	5.88	6.28		6.9	−0.7	−1.5

[a] Compounds designated by asterisk were studied in this work for the first time.
[b] Superscript numbers in brackets indicate references from which UPS data were taken. The available Hammett constants were taken from [19].

atom. Nonetheless, the correlation between chemical shifts and Fe3d a_1' σ-type orbital is worse than for Fe3d e_2' δ-type orbital (Table 4). This suggests that metal–ligand δ-bonding is stronger than σ-type bonding. This is in accord with the interpretation of bonding in ferrocene deduced from DFT calculations which showed that bonding contributions of Fe3d δ- and σ-orbitals are 29.7% and 6.4%, respectively [21]. Another important deduction from Table 4 concerns correlations between substituent constants and Fe3d and π_2 and π_1-orbital ionization energies. Fe3d energies correlate better with substituent constants than do π_2 and π_1 energies. How can we explain this trend?

The trend is consistent with the proposed description of bonding in ferrocene which suggested that the main bonding mechanism is Fe3d ← Cp π-donation [21]. Partial transfer of frontier electron density from ligand to metal makes the energy levels of the latter more sensitive to

Table 4
Linear regression analysis of molecular descriptors

	δ(ppm)	$\Sigma\sigma^+$	$\Sigma\sigma^-$	$\Sigma\sigma_m$	$\Sigma\sigma_p$
⟨3d⟩	SD = 0.2 R = 0.53				
3d (a_1')	SD = 129.9 R = 0.48	SD = 0.36 R = 0.90	SD = 0.36 R = 0.90	SD = 0.22 R = 0.82	SD = 0.23 R = 0.91
3d (e_2')	SD = 123.2 R = 0.55	SD = 0.33 R = 0.92	SD = 0.48 R = 0.81	SD = 0.22 R = 0.85	SD = 0.20 R = 0.93
⟨π_2⟩		SD = 0.27 R = 0.66	SD = 0.44 R = 0.31	SD = 0.32 R = 0.73	SD = 0.30 R = 0.77
⟨π_1⟩		SD = 0.21 R = 0.74	SD = 0.48 R = 0.32	SD = 0.26 R = 0.80	SD = 0.83 R = 0.83

substituent effects and hence leads to better correlation with Hammett substituent constants.

Our correlation analysis provides further insights into the nature of metal–ligand bonding in ferrocenes. Metal and ligand ionization energies correlate better with σ_p than with σ_m constants (Table 4). σ_m constants account mostly for inductive interactions between substituent and the aromatic ring while σ_p account for both inductive and resonance effects [19]. This suggests that Fe–Cp interactions are not exclusively of Fe ← Cp π-dative type. This observation is based on experimental values alone, but it is nonetheless consistent with the computational results which claimed that metal–ligand bonding in ferrocene is approximately 50% electrostatic (ionic) and 50% covalent in nature [21]. The final comment demonstrates the sensitivity of our correlation method to (non)bonding orbital characters. σ^+/σ^- constants describe interaction between positively/negatively charged reaction centre and the substituent which can interact with it via MO resonance effect. In our case, the "reaction centre" can be considered as a positive hole created upon photoionization and residing mostly on the atom where ionized orbital has the highest density. This comment explains why Fe3d a_1' energies correlate equally well with σ^+ and σ^- constants, while Fe3d e_2' energies correlate better with σ^+ than with σ^- constants. Fe3d a_1' orbital is less bonding than e_2' (see above) and thus interaction between the positive hole at iron atom and the substituents at Cp ring will be reduced. On the other hand, Fe3d e_2' orbital is more bonding [21] and thus its ionization energies correlate better with σ^+ than with σ^- values.

4. Conclusion

We used a combination of experimental measurements to analyze the nature of metal–ligand bonding in ferrocenes by performing correlation analysis of molecular descriptors. We conclude on the basis of experimental evidence alone, that metal–ligand bonding in ferrocene must include covalent, (Fe ← Cp) π-back-donation type bonding as well as ionic (electrostatic) contribution comprising charged Fe^{2+} and $(Cp^-)_2$ fragments. Such description of metal–ligand bonding has been put forward on the basis of DFT calculations [21], but due to the inevitable dependence of theoretical results on model Hamiltonian and basis sets it is important to independently substantiate theoretical claims by experimentally derived quantities.

References

[1] R.C.J. Atkinson, V.C. Gibson, N.J. Long, Chem. Soc. Rev. 33 (2004) 213.
[2] G. Fronzoni, P. Colavita, M. Stener, G. De Alti, P. Decleva, J. Phys. Chem. A 105 (2001) 9800.
[3] K. Ishimura, M. Hada, H. Nakatsuji, J. Chem. Phys. 117 (2002) 6533.
[4] D.L. Lichtenberger, N.E. Gruhn, S.K. Renshaw, J. Mol. Struct. 405 (1997) 79.
[5] C. Cauletti, J.C. Green, M.R. Kelly, P. Powell, J. Van Tilborg, J. Robbins, J. Smart, J. Electron. Spectrosc. Relat. Phenom. 19 (1980) 327.
[6] T. Vondrak, J. Organomet. Chem. 275 (1984) 93.
[7] T. Vondrak, J. Organomet. Chem. 306 (1986) 89.
[8] T. Matsumura-Inoue, K. Kuroda, Y. Umezawa, Y. Achiba, J. Chem. Soc. Faraday Trans. 2 85 (1989) 857.
[9] Z.V. Todres, A.I. Safronov, D.S. Ermekov, R.M. Minyaev, J. Organomet. Chem. 441 (1992) 479.
[10] J.C. Green, P. Decleva, Coord. Chem. Rev. 249 (2005) 209.
[11] D.L. Lichtenberger, H.J. Fan, N.E. Gruhn, J. Organomet. Chem. 666 (2003) 75.
[12] (a) S. Barlow, M.J. Drewitt, T. Dijkstra, J.C. Green, D. O'Hare, C. Whittingham, H.H. Wynn, D.P. Gates, I. Manners, J.M. Nelson, J.K. Pudelski, Organometallics 17 (1998) 2113;
(b) K. Kimura, S. Katsumata, Y. Achiba, T. Yamazaki, S. Iwata, Handbook of HeI Photoelectron Spectra of Fundamental Organic Molecules, Japan Scientific Societies Press, Tokyo, 1981.
[13] M.J. Frisch, G.W. Trucks, H.B. Schlegel, G.E. Scuseria, M.A. Robb, J.R. Cheeseman, V.G. Zakrzewski, J.A. Montgomery Jr., R.E. Stratmann, J.C. Burant, S. Dapprich, J.M. Millam, A.D. Daniels, K.N. Kudin, M.C. Strain, O. Farkas, J. Tomasi, V. Barone, M. Cossi, R. Cammi, B. Mennucci, C. Pomelli, C. Adamo, S. Clifford, J. Ochterski, G.A. Petersson, P.Y. Ayala, Q. Cui, K. Morokuma, D.K. Malick, A.D. Rabuck, K. Raghavachari, J.B. Foresman, J. Cioslowski, J.V. Ortiz, B.B. Stefanov, G. Liu, A. Liashenko, P. Piskorz, I. Komaromi, R. Gomperts, R.L. Martin, D.J. Fox, T. Keith, M.A. Al-Laham, C.Y. Peng, A. Nanayakkara, C. Gonzalez, M. Challacombe, P.M.W. Gill, B. Johnson, W. Chen, M.W. Wong, J.L. Andres, C. Gonzalez, M. Head-Gordon, E.S. Replogle, J.A. Pople, GAUSSIAN 03, Revision B.05, Gaussian, Inc., Pittsburgh, PA, 2003.
[14] M. Dolg, Mol. Phys. 88 (1996) 1645.
[15] M.M. Coutiere, J. Demuynck, A. Veillard, Theor. Chim. Acta 27 (1972) 281.
[16] J.J. Yeh, Atomic Calculation of Photoionization Cross-sections and Asymmetry Parameters, Grodon & Breach, Langhorne, 1993.
[17] H. Haslinger, K. Koci, W. Robien, K. Schlogl, Monatsh Chem. 114 (1983) 495.
[18] B. Wrackmeyer, A. Ayazi, H.E. Maisel, M. Herberhold, J. Organomet. Chem. 630 (2001) 263.
[19] A. Williams, Free Energy Relationships in Organic and Bioorganic Chemistry, Royal Society of Chemistry, Cambridge, 2003.
[20] W. Philipsborn, Chem. Soc. Rev. 28 (1999) 95.
[21] V.M. Rayon, G. Frenking, Organometallics 22 (2003) 3304.